

## WRINKLED MEMBRANES

**Y.W. Wong and S. Pellegrino**

*Department of Engineering*

*University of Cambridge*

*Trumpington Street, Cambridge, CB2 1PZ, U.K.*

*Email: [pellegrino@eng.cam.ac.uk](mailto:pellegrino@eng.cam.ac.uk)*

*Web page: <http://www-civ.eng.cam.ac.uk/dsl/index.html>*

**Key words:** Membranes, Thin Shells, Wrinkles.

**Abstract.** *This paper investigates the wrinkling of square isotropic membranes subject to coplanar pairs of equal and opposite corner forces. These membranes are initially stress free and perfectly flat. Two wrinkling regimes are observed experimentally and are also reproduced by means of finite-element simulations. A general methodology for making preliminary analytical estimates of wrinkle patterns and average wrinkle amplitudes and wavelengths, while also gaining physical insight into the wrinkling of membranes, is presented.*

## 1 INTRODUCTION

Thin, prestressed membranes will be required for the next generation of spacecraft, to provide deployable mirror surfaces, solar collectors, sunshields, solar sails, etc. Some applications require membranes that are perfectly smooth in their operational configuration; other applications can tolerate membranes that are wrinkled with a known, small deviation from the nominal shape. Because the design of membrane structures with biaxial pretension, which have a smooth surface, significantly increases the overall complexity of the structure, for those applications in which sufficiently small wrinkles are acceptable, engineers need to estimate the extent, wavelength and amplitude of the wrinkles.

The wrinkling of membranes has attracted much interest in the past, starting from the development of the tension field theory.<sup>1</sup> Simpler formulations and extensions of this theory were later proposed.<sup>2–7</sup> All of these formulations, with accompanying numerical solutions,<sup>8,9</sup> model the membrane as a *no-compression, two-dimensional continuum with negligible bending stiffness*. Several studies of membrane wrinkling have been carried out during the past three years, and have been presented at the 42nd, 43rd, and 44th AIAA SDM Conferences.<sup>10–12</sup>

This paper considers a uniform elastic square membrane (which is a simple model of a square solar sail) of side length  $L$  and thickness  $t$  that is prestressed by two pairs of equal and opposite concentrated forces,  $T_1$  and  $T_2$ , uniformly distributed over a small length  $d$  at the corners, as shown in Figure 1. This membrane is isotropic with Young's Modulus  $E$  and Poisson's ratio  $\nu$ ; it is also initially stress free and perfectly flat (before the application of the corner forces).

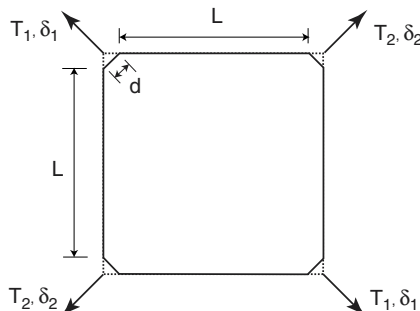


Figure 1: Membrane subjected to corner forces.

We use this problem to present a general and yet simple analytical method for making preliminary estimates of wrinkle patterns and average wrinkle amplitudes and wavelengths in membrane structures. We also present a finite element simulation method for making more accurate estimates. The results from both our analytical approach and finite element simulations are compared with experimental measurements.

The paper's layout is as follows. Section 2 describes two regimes of wrinkling that were observed experimentally. Section 3 presents our methodology for tackling wrinkling problems analytically, and hence derives solutions for the square membrane problem. Section 4 presents a finite-element simulation technique, whose results are compared with measurements and analytical results in Section 5. Section 6 concludes the paper.

## 2 EXPERIMENTAL OBSERVATIONS

Figure 2 shows photographs of the wrinkle patterns in a Kapton membrane with  $L = 500$  mm,  $t = 0.025$  mm, and  $d = 25$  mm. For symmetric loading ( $T_1 = T_2$ ), Figure 2(a), the wrinkle pattern is fairly symmetric, with wrinkles radiating outward from each corner; the central region is free of wrinkles. For a load ratio of  $T_1/T_2 = 2$  the wrinkles grow in amplitude but remain concentrated at the corners. Then, for  $T_1/T_2 = 3$  a large diagonal wrinkle becomes visible, whose amplitude grows further for  $T_1/T_2 = 4$ .

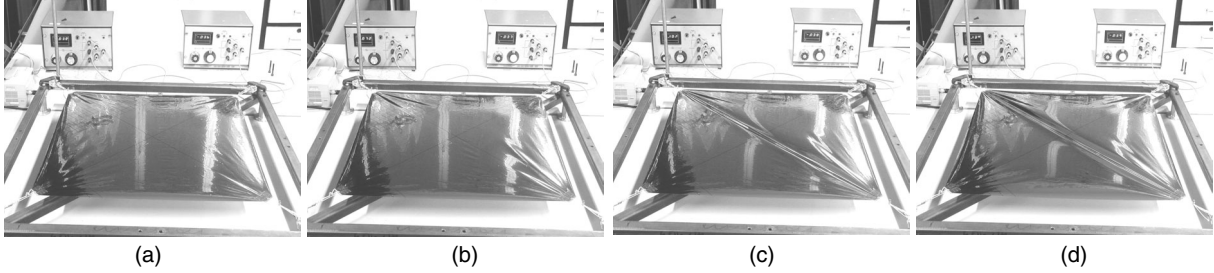


Figure 2: Wrinkled shapes for  $T_1$  equal to (a) 5 N, (b) 10 N, (c) 15 N, and (d) 20 N;  $T_2 = 5$  N in all cases.

## 3 ANALYTICAL APPROACH

Our analytical approach is in four parts, as follows.

First, we identify a two-dimensional stress field that involves no compression anywhere in the membrane; the regions where the minor principal stress is zero are then assumed to be wrinkled and the wrinkles are assumed to be along the major principal stress directions. Ideally, both equilibrium and compatibility should be satisfied everywhere by the selected stress field, but analytical solutions in closed-form —obtained by tension field theory— exist only for very simple boundary conditions. We have recently shown<sup>13</sup> that a carefully chosen, simple stress field that satisfies only equilibrium can provide quick solutions that are useful for preliminary design. More accurate stress fields can be obtained from a two-dimensional stress analysis with membrane finite elements, as briefly discussed in Section 4.

Second, we note that the bending stiffness of the membrane is finite, although small, and hence a compressive stress will exist in the direction perpendicular to the wrinkles. Because of its small magnitude, this stress was neglected in our previous analysis of the stress field. We assume that this compressive stress varies only with the wavelength of the wrinkles and set it equal to the critical buckling stress of a thin plate in uniaxial compression. Thus, the stress across the wrinkles is a known function of the wrinkle wavelength.

Third, we enforce equilibrium in the out-of-plane direction. Since the stress distribution is known, except for the wrinkle wavelength, a single equation of equilibrium will determine the wrinkle wavelength.

Fourth, the wrinkle amplitudes are estimated by considering the total strain in the membrane as the sum of two components, a material strain and a wrinkling strain.

### 3.1 Stress Field

Figure 3 shows three equilibrium stress fields that can be used to analyse membranes under (a) a symmetric loading, (b) an asymmetric loading with  $T_1/T_2 \leq 1/(\sqrt{2} - 1)$ , and (c) an

asymmetric loading with  $T_1/T_2 \geq 1/(\sqrt{2}-1)$ . In each case the membrane is divided into regions which are subject to simple stress states.

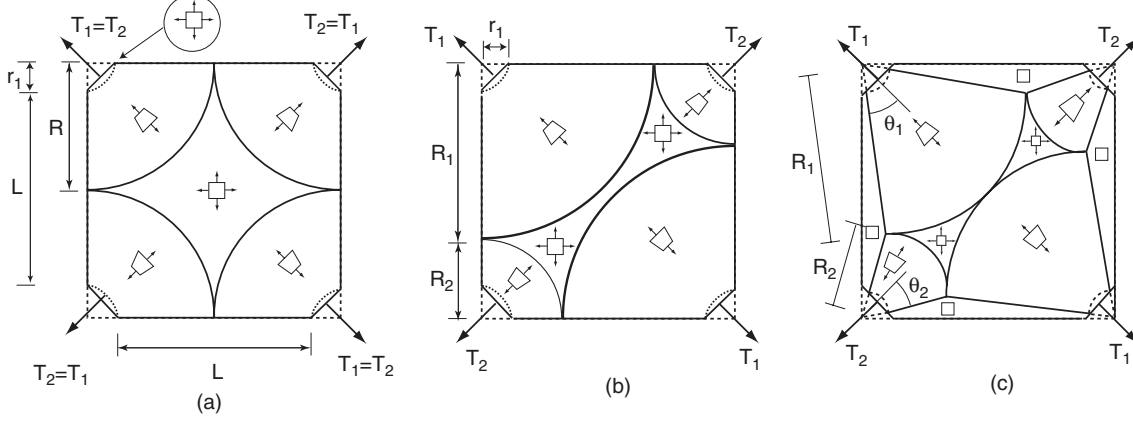


Figure 3: Stress fields.

The stress field in Figure 3(a) is purely radial in the corner regions, with

$$\sigma_r = \frac{T}{\sqrt{2}rt} \quad (1)$$

where  $r < \frac{L}{2}$  is the radial distance measured from the apex. Hence,  $\sigma_r$  is uniform on any circular arc and all other stress components are zero. The central region, defined by circular arcs of radius  $R = r_1 + L/2$ , is subject to uniform biaxial stress of magnitude  $T/\sqrt{2}Rt$ .

Note that near the point of application of each corner load a small, biaxially stressed region bounded by the radius  $r_1 = \frac{d}{\sqrt{2}}$  has been defined. In these regions both normal stress components are given by  $T/dt$ .

For moderately asymmetric loading, see Figure 3(b), we consider corner stress fields similar to those given by Equation 1, hence

$$\sigma_r = \frac{T_i}{\sqrt{2}rt} \quad (2)$$

but vary the outer radii such that the radial stress is still uniform on the four arcs bounding the central region. Hence we need to choose  $R_1$  and  $R_2$  such that  $R_1/R_2 = T_1/T_2$  and  $R_1 + R_2 = L + 2r_1$ . This approach is valid until the two larger arcs reach the centre of the membrane, which happens for

$$\frac{R_1}{R_2} = \frac{T_1}{T_2} = \frac{1}{\sqrt{2}-1} \quad (3)$$

For larger values of  $T_1/T_2$  we consider the stress field shown in Figure 3(c); note that the diagonal region between the two most heavily loaded corners of the membrane is subject to zero transverse stress, and hence a single diagonal wrinkle can form. Also note that the edges of the membrane are now unstressed. The stress in each corner region is now given by

$$\sigma_r = \frac{T_i}{2rt \sin \theta_i} \quad (4)$$

and hence for the central region to be biaxially stressed we need to satisfy the condition

$$\sigma_r = \frac{T_1}{2R_1 t \sin \theta_1} = \frac{T_2}{2R_2 t \sin \theta_2} \quad (5)$$

Given  $T_1$  and  $T_2$ , one can find —by geometry together with Equation 5— a unique set of values for the half-angles defining the corner regions,  $\theta_1, \theta_2$ , and for the radii,  $R_1, R_2$ , thus fully defining the stress field.

The values of  $\theta_1$  and  $\theta_2$  remain constant for any particular value of  $T_1/T_2$ , and so the only variable in Equation 4 is  $r$ . Hence, the slack regions will grow as the load ratio is increased. Finally, it should be noted that both of our earlier stress fields can be obtained as special cases of the last one.

### 3.2 Wrinkle Details

A critical compressive stress,  $\sigma_{cr}$ , must exist in the direction transverse to the wrinkles. We will assume that this stress is given by the buckling stress of an infinitely long plate of width  $\lambda$

$$\sigma_{cr} = -\frac{\pi^2}{\lambda^2} \frac{Et^2}{12(1-\nu^2)} \quad (6)$$

In the case of fan-shaped wrinkles we will set  $\lambda$  equal to the half-wavelength mid way between the corner and the edge of the fan.

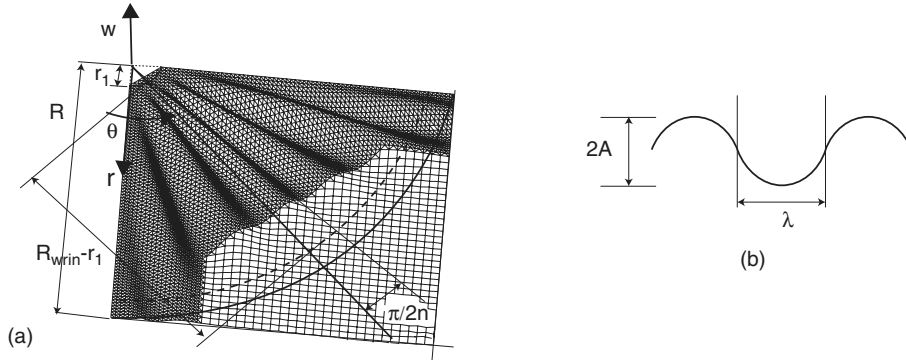


Figure 4: Corner wrinkles: (a) overall shape; (b) central cross section.

To estimate the wrinkle details, we begin by considering a simple analytical expression for the wrinkled surface. For example, in the case of a symmetrically loaded membrane we assume that at each corner there is a set of uniform, radial wrinkles whose out-of-plane shape can be described in the polar coordinate system of Figure 4 by

$$w = A \sin \frac{\pi(r - r_1)}{R_{wrin} - r_1} \sin 2n\theta \quad (7)$$

where  $A$  is the wrinkle amplitude,  $n$  the total number of wrinkles at the corner —each subtending an angle of  $\pi/2n$ — and  $\theta$  is an angular coordinate measured from the edge of the membrane.

Since the stress in the corner regions is uniaxial there is the possibility of wrinkles forming there. The radial strain is

$$\epsilon_r = \sigma_r/E \quad (8)$$

where  $\sigma_r$  is given by Equation 1. The corresponding radial displacement,  $u(r)$  (positive outwards), can be obtained from

$$u = \int \epsilon_r dr + c \quad (9)$$

where the constant of integration  $c$  can be obtained by noting that  $u \approx 0$  at  $r = R$ , i.e. at the edge of the biaxially stressed region. Therefore,

$$u = \frac{T}{\sqrt{2}Et} \ln \frac{r}{R} \quad (10)$$

The hoop strain required for geometric compatibility is

$$\epsilon_{\theta_g} = \frac{u}{r} \quad (11)$$

and the hoop material strain is

$$\epsilon_{\theta_m} = -\nu \frac{\sigma_r}{E} \quad (12)$$

Wrinkles will form when  $\epsilon_{\theta_g}$  is larger in magnitude than  $\epsilon_{\theta_m}$  (note that both strains are negative), hence combining Equations 1, 10–12, we obtain

$$\ln \frac{R}{r} \geq \nu \quad (13)$$

The radius of the wrinkled region,  $R_{\text{wrin}}$ , is the largest  $r$  for which Equation 13 is satisfied. Within the wrinkled region, i.e. for  $r < R_{\text{wrin}}$ , an additional “wrinkling” strain is required

$$\epsilon_{\theta_g} = \epsilon_{\theta_m} + \epsilon_{\theta_{\text{wrin}}} \quad (14)$$

The wrinkling strain is related to the wrinkle amplitude, and for the wrinkle shape defined by Equation 7 it can be shown that at  $r = (R_{\text{wrin}} - r_1)/2$

$$\epsilon_{\theta_{\text{wrin}}} = -\frac{\pi^2 A^2}{4\lambda^2} \quad (15)$$

Substituting Equation 10 into Equation 11 and Equation 1 into Equation 12, and then both into Equation 14 we find that  $A$  has to satisfy

$$\frac{\sqrt{2}T}{Et(R_{\text{wrin}} - r_1)} \ln \frac{R_{\text{wrin}} - r_1}{2R} = -\frac{\sqrt{2}\nu T}{Et(R_{\text{wrin}} - r_1)} - \frac{\pi^2 A^2}{4\lambda^2} \quad (16)$$

Next, we work out the number of wrinkles by considering out-of-plane equilibrium of the wrinkled membrane at a point of maximum out-of-plane displacement, e.g. at  $r = (R_{\text{wrin}} - r_1)/2, \theta = \pi/4n$ . The equilibrium equation is

$$\sigma_r \kappa_r + \sigma_\theta \kappa_\theta = 0 \quad (17)$$

where  $\kappa_r$  and  $\kappa_\theta$  are the curvatures in the radial and hoop directions, respectively, which can be obtained by differentiating Equation 7. Hence,

$$\kappa_r = -\frac{A\pi^2}{(R_{\text{wrin}} - r_1)^2} \quad \text{and} \quad \kappa_\theta = -\frac{16An^2}{(R_{\text{wrin}} - r_1)^2} \quad (18)$$

The transverse stress component  $\sigma_\theta$  is set equal to  $\sigma_{\text{cr}}$ . Substituting Equations 1, 6 and 18 into Equation 17 gives

$$\frac{\sqrt{2}T}{(R_{\text{wrin}} - r_1)t} - \frac{4Et^2n^2}{3(1 - \nu^2)\lambda^2} = 0 \quad (19)$$

Since  $\lambda$  is related to the number of wrinkles by

$$\lambda = \frac{R_{\text{wrin}} - r_1}{2} \frac{\pi}{2n} \quad (20)$$

we can substitute for  $\lambda$  into Equation 19 and solve for  $n$  to obtain

$$n = \sqrt[4]{\frac{3\sqrt{2}\pi^2T(R_{\text{wrin}} - r_1)(1 - \nu^2)}{64Et^3}} \quad (21)$$

Given Equations 20 and 21 we can predict the wrinkle amplitude  $A$  by solving Equation 16, which gives

$$A = \frac{2\lambda}{\pi} \sqrt{\frac{\sqrt{2}T}{Et(R_{\text{wrin}} - r_1)} \left( \ln \frac{2R}{R_{\text{wrin}} - r_1} - \nu \right)} \quad (22)$$

In the case  $T_1 \neq T_2$  it is straightforward to generalize Equations 19 and 22 to find the wavelength and amplitude of the wrinkles in each corner region. However, for  $T_1/T_2 \geq 1/(\sqrt{2}-1)$  the two larger corner stress fields come into contact, see Figure 3(c), and hence a single diagonal wrinkle can form between the two most heavily loaded corners. This much larger wrinkle can be analysed following a similar approach<sup>13</sup> to obtain the following expressions for half-wavelength and amplitude

$$\lambda = \sqrt[4]{\frac{2\pi^2R_1(R_1 - r_1)^2Et^3 \sin \theta_1}{3(1 - \nu^2)T_1}} \quad (23)$$

and

$$A = \frac{2\sqrt{\lambda(\delta_1 + \delta_2)}}{\pi} \quad (24)$$

Here  $\delta_1$  and  $\delta_2$  are the radial displacements of the corners loaded by  $T_1$  and  $T_2$ , respectively; these corner displacements can be estimated from

$$\delta_i \approx \frac{T_i}{2Et \sin^2 \theta_i} \left[ \theta_i \ln \left| \frac{R_i}{r_1} \right| + (1 - \nu) \left( \frac{A}{R_i^2} + \theta_i - \frac{1}{2} \tan \theta_i \right) \right] \quad i = 1, 2 \quad (25)$$

More refined estimates can be obtained from a two-dimensional finite-element analysis, see Section 5.

## 4 FINITE-ELEMENT SIMULATIONS

We have recently shown<sup>14</sup> that wrinkling of a thin membrane can be accurately modelled using the thin shell elements available in the commercial finite-element package ABAQUS.<sup>15</sup> The analysis is carried out by introducing initial geometrical imperfections, obtained from an initial eigenvalue analysis, followed by a geometrically non-linear post-buckling analysis using the pseudo-dynamic \*STABILIZE solution scheme. This approach, although expensive in computational terms, is so far the only method that can reveal full wrinkle details and can be relied upon as an almost exact replication of physical experimentation. An alternative approach is the Iterative Modified Properties (IMP) method<sup>9</sup> which uses a combined stress-strain wrinkling criterion in a two-dimensional membrane model. The IMP method has been recently implemented as an ABAQUS user subroutine and has been shown to accurately predict the extent of the wrinkled regions and the two-dimensional stress distribution—but of course not the details of the wrinkles.

Both of these modelling techniques were used to simulate a 0.025 mm thick,  $500 \times 500$  mm<sup>2</sup> square Kapton membrane ( $E=3530$  N/mm<sup>2</sup> and  $\nu = 0.3$ ). The membrane was loaded at each corner through a spreader beam by a 0.1 mm thick, 25 mm  $\times$  20 mm Kapton tabs—as in the experiment of Section 2.

A uniform mesh of 200 by 200 square elements was used to model the whole structure, in order to capture the fine wrinkle details in the corners.

In the shell model, the Kapton membrane and the corner tabs were modelled using S4R5 thin shell elements of different thickness. At the corners, the shell elements were connected to “Circ” beam elements through the \*MPC, TIE function. The central node was constrained against translation in the  $x$ - and  $y$ -direction; all side edges were left free. Both the out-of-plane rotations of the membrane and all in-plane bending degrees of freedom of the corner beams were restrained. The corner loads were applied as distributed loads along the truncated corners of the membrane.

In the IMP model, the membrane was modelled using M3D4 membrane elements, whose constitutive behaviour was modelled through a UMAT subroutine. The corner tabs were modelled with S4 shell elements and the same beam elements as for the shell model were used.

### 4.1 Simulation Details

Two load steps were applied, first a symmetric loading of  $T_1 = T_2 = 5$  N. Second,  $T_2 = 5$  N was maintained while  $T_1$  was increased up to 20 N.

The analysis procedure was essentially identical for all of the simulations. First, a uniform prestress of 0.5 N/mm<sup>2</sup> was applied, to provide initial out-of-plane stiffness to the membrane. This was achieved by means of \*INITIAL CONDITION, TYPE=STRESS. Next, a non-linear-geometry analysis was carried out, with \*NLGEOM, to check the equilibrium of the prestressed system. Then, a linear eigenvalue analysis step was carried out (for the thin shell model only) in order to extract possible wrinkling mode-shapes of the membrane under a symmetrical loading. Four such mode-shapes were selected, based on their resemblance to the expected final wrinkled shape, and were introduced as initial geometrical imperfections. Finally, an automatically stabilised post-wrinkling analysis was performed, with \*STATIC, STABILIZE. This analysis is very sensitive because the magnitude of the wrinkles is very small, hence an increment of 0.001 of the total load had to be selected. The default stabilize factor was reduced to  $10^{-12}$  to minimise the amount of fictitious damping; this was the smallest amount required to stabilise the solution.

Figure 5(a) shows the symmetrically wrinkled shape obtained for  $T_1 = T_2 = 5$  N. The wrinkle amplitudes are very small and have been enlarged 100 times for clarity. Figure 5(b) shows the



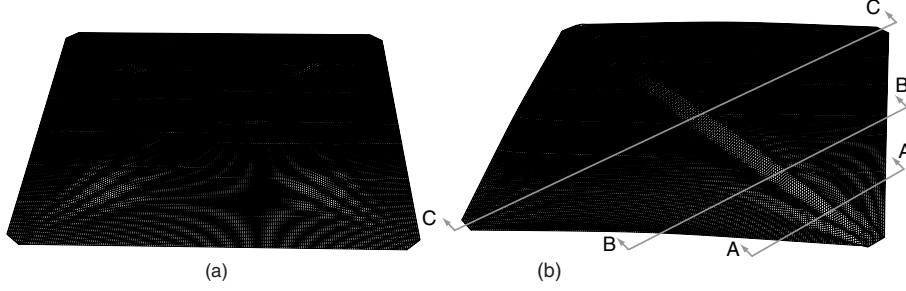


Figure 5: Wrinkled shapes for (a)  $T_1/T_2 = 1$  and (b)  $T_1/T_2 = 4$ .

corresponding shape for  $T_1/T_2 = 4$ . Here the distinguishing feature is a large diagonal wrinkle between the two more heavily loaded corners, a number of smaller wrinkles can also be seen near the corners with smaller loads.

Figure 6 shows the wrinkle profiles measured at three different cross sections, for  $T_1/T_2 = 4$ , plotted against those obtained from the simulations. Note that experiments and simulations match closely in the central region; the wrinkle wavelengths, in particular, are predicted quite accurately. But ABAQUS predicts smaller displacements of the edges of the membrane, due to the fact that the initial shape of the physical model has not been captured with sufficient accuracy (the edges of a Kapton sheet are naturally curled).

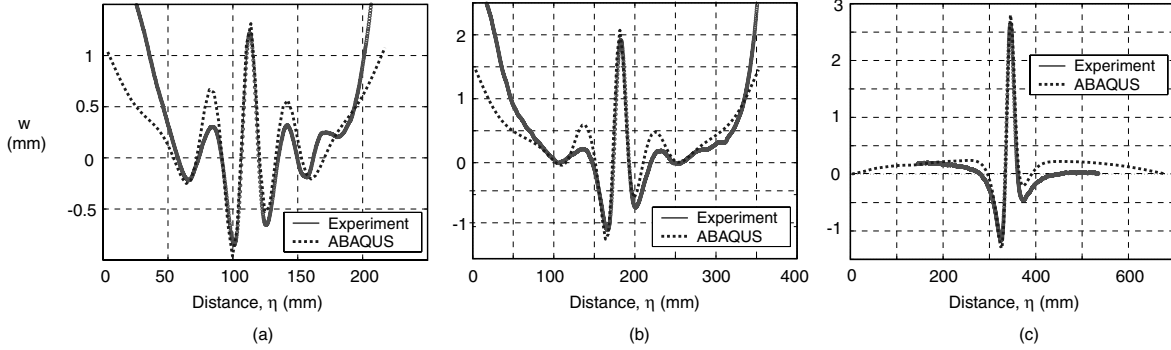


Figure 6: Comparison of experimental measurements with ABAQUS results for  $T_1/T_2 = 4$  and for cross sections at distance of (a) 105 mm, (b) 177 mm, (c) 346 mm from corner.

## 5 VALIDATION OF ANALYTICAL AND FINITE-ELEMENT MODELS

Table 1 compares the predicted wrinkle half-wavelengths and amplitudes from Equations 20–22 with experimental measurements for a symmetrically loaded membrane, i.e. for  $T_1/T_2 = 1$ .

For the load case  $T_1/T_2 = 4$ , Table 2 compares the analytical predictions for the large diagonal wrinkle at the centre of the membrane, for two different membrane thicknesses, with predictions from ABAQUS and experimental measurements. The wavelength predictions are very close. The wrinkle amplitudes have been estimated first using only analytical solutions, Equation 24 with  $\delta_1$  and  $\delta_2$  from Equation 25, and second using Equation 24 but with corner deflections

$T$ (N)	$n$		$\lambda$ at $r = 70$ mm		$A$	
	Eq. 21	Exp.	Eq. 20	Exp.	Eq. 22	Exp.
5	9.6	8	11.6	11.0	0.16	0.12
20	13.6	11	8.3	9.7	0.22	0.14

Table 1: Wrinkles under symmetric loading (all dimensions in mm)

$t$	$\lambda$			$A$			
	Eq. 23	Exp.	FE	Eqs 24, 25	Eq. 24+FE <sup>4</sup>	Exp.	FE <sup>5</sup>
0.025	24.6	23.8	22.3	3.5	2.8	1.9	2.0
0.050	41.3	33.9	35.6	3.2	2.1	1.8	1.6

Table 2: Wrinkle half-wavelengths and amplitudes for  $T_1/T_2 = 4$  at  $r = 346$  (all dimensions in mm)

from a 2-D IMP analysis. We can see that the fully analytical estimates are up to 88% higher than those measured experimentally, but if we use the corner displacements from the 2D finite-element analysis we obtain estimates that are only 48% and 16% higher than the measurements.

## 6 DISCUSSION AND CONCLUSIONS

The wrinkling of square membranes subject to coplanar pairs of equal and opposite corner forces has been investigated. It has been shown that two wrinkling regimes exist. The first regime occurs for symmetric loading and asymmetric loading up to approximately  $T_1/T_2 = 2.41$ , and it is characterised by relatively small, radial corner wrinkles. The second regime occurs for asymmetric loading with approximately  $T_1/T_2 > 2.41$ , and is characterised by a single, large diagonal wrinkle, plus small radial wrinkles at all four corners. Each regime has been observed experimentally and also reproduced to great accuracy in a finite-element simulation.

A general methodology for gaining insight into the wrinkling of membranes, which was first proposed for uniformly wrinkled membranes in shear,<sup>16</sup> has been presented. For the first wrinkling regime ( $T_1/T_2 < 2.41$ ) it is reasonable to assume uniform, fan-shaped wrinkles expressed in terms of sine functions. With these assumptions, analytical expressions have been derived for the number of corner wrinkles and their average maximum amplitude. For the second wrinkling regime ( $T_1/T_2 > 2.41$ ) an analogous derivation leads to an expression for the amplitude of the central wrinkle. These expressions have been found to overestimate wrinkle amplitudes by up to 50%, and hence they appear to be sufficiently accurate for preliminary design.

Finite element analysis using thin shell elements has been shown to be able to replicate real physical experimentation with an accuracy typically better than 10% on amplitude. However, a very fine mesh had to be used to resolve the small corner wrinkles; hence a complete simulation takes up to several days on a 2GHz Pentium 4 PC.

---

<sup>4</sup>Membrane model with IMP.

<sup>5</sup>Shell model.

## 7 ACKNOWLEDGMENTS

We thank Professors C.R. Calladine and K.C. Park for helpful suggestions. Partial support from NASA Langley Research Center, research grant NAG-1-02009, Integrated membranous-microelement space structures technology (technical monitor Dr K. Belvin) is gratefully acknowledged.

## REFERENCES

- [1] H. Wagner. Flat sheet metal girder with very thin metal web, *Zeitschrift für Flugtechnik Motorluftschiffahrt*. **20**, 200–207, 227–233, 256–262, 279–284 (1929).
- [2] E. Reissner. On tension field theory. *Proc. 5th Int. Cong. Appl. Mech.*, 88–92 (1938).
- [3] M. Stein and J.M. Hedgepeth. *Analysis of Partly Wrinkled Membranes*. NASA Langley Research Center, NASA TN D-813 (1961).
- [4] E.H. Mansfield. Tension field theory a new approach which shows its duality with inextensional theory. *Proc. 12th Int. Cong. Appl. Mech.*, 305–320 (1969).
- [5] E.H. Mansfield. *The Bending and Stretching of Plates*, second edition. Cambridge University Press, Cambridge (1989).
- [6] A.C. Pipkin. The relaxed energy density for isotropic elastic membranes. *IMA J. Appl. Math.*, **36** 85–99 (1986).
- [7] M. Epstein and M.A. Forcinito. Anisotropic membrane wrinkling: theory and analysis. *Int. J. Solids Structures*. **38**, 5253–5272 (2001).
- [8] C. Jenkins and J.W. Leonard. Nonlinear dynamic response of membranes: State of the art. *ASME Appl. Mech. Reviews*, **44**, 319–328 (1991).
- [9] A. Adler. *Finite Element Approaches for Static and Dynamic Analysis of Partially Wrinkled Membrane Structures*. Ph.D. Dissertation, University of Colorado at Boulder (2000).
- [10] *Proc. 42nd AIAA/ASME/ASCE/AHS/ASC Structures, Structural Dynamics and Materials Conference*, 16–19 April 2001, Seattle, WA, AIAA, Reston (2001).
- [11] *Proc. 43rd AIAA/ASME/ASCE/AHS/ASC Structures, Structural Dynamics, and Materials Conference and Exhibit*, Denver, CO, 22–25 April 2002, AIAA, Reston (2002).
- [12] *Proc. 44th AIAA/ASME/ASCE/AHS/ASC Structures, Structural Dynamics, and Materials Conference and Exhibit*, Norfolk, VA, 7–10 April 2003, AIAA, Reston (2003).
- [13] Y.W. Wong, S. Pellegrino, and K.C. Park. Prediction of wrinkle amplitudes in square solar sails. *Proc. 44th AIAA/ASME/ASCE/AHS/ASC Structures, Structural Dynamics, and Materials Conference and Exhibit*, Norfolk, VA, 7–10 April 2003, AIAA-2003-1982 (2003).
- [14] Y.W. Wong and S. Pellegrino. Computation of wrinkle amplitudes in thin membranes. *Proc. 43rd AIAA/ASME/ASCE/AHS/ASC Structures, Structural Dynamics, and Materials Conference and Exhibit*, Denver, CO, 22–25 April 2002, AIAA-2002-1369 (2002).

- [15] Hibbit, Karlsson and Sorensen, Inc., *ABAQUS Theory and Standard User's Manual*, Version 6.2, Pawtucket, RI, USA (2001).
- [16] Y.W. Wong and S. Pellegrino. Amplitude of wrinkles in thin membranes. In: *New Approaches to Structural Mechanics, Shells and Biological Structures*, edited by H.R. Drew and S. Pellegrino. Kluwer Academic Publishers, 257-270 (2002).